



## Modelling the effect of depth, width, and velocity of tillage tine on soil stress and draught using the finite element method

Meysam Latifi Amoghini<sup>1</sup>, Gholamhossein Shahgholi<sup>1\*</sup>, Agata Dziwulska-Hunek<sup>2</sup> , Mariusz Szymanek<sup>3</sup> 

<sup>1</sup>Department of Biosystem Engineering, University of Mohaghegh Ardabili, Ardabil 56199-11367, Iran

<sup>2</sup>Department of Biophysics, University of Life Sciences in Lublin, Akademicka 13, 20-950 Lublin, Poland

<sup>3</sup>Department of Agricultural, Forest and Transport Machinery, University of Life Sciences in Lublin, Głęboka 28, 20-612 Lublin, Poland

Received March 19, 2024; accepted November 13, 2024

**Abstract.** Four types of narrow tines with different widths but the same length of 1 m were analysed. Field trials were conducted in clay loam soil in a factorial experiment based on a randomized complete block design with three replications. The soil moisture was 15%, and four tractor forward speeds of 1, 1.5, 1.8, and 3 km h<sup>-1</sup> and tine widths of 2.5, 3, 3.5, and 4 cm at working depths of 10, 20, 30, and 40 cm were investigated relative to the required draught. In order to investigate the effect of the depth/width ratio and the speed of the narrow tillage blade on the draught force, a three-dimensional model was prepared and tested at different settings. The results of the draught force applied to the blade were recorded. Increasing the forward speed showed a significant effect on increasing the stress exerted on the soil, but increasing the depth/width ratio reduced the stress created in the soil. It was found that the forward speed, tilling depth, and tine width increment exerted a significant effect on increasing the required draught.

**Keywords:** narrow tine, abaqus, finite element method, Drucker-Prager, depth/width ratio

### 1. INTRODUCTION

Tillage has always been and will be an integral part of crop production. It has many roles in crop production, including seed bed preparation, seed placement, nutrient incorporation and other amendments, and water and pest management (Lobb *et al.*, 2007). Seed germination and crops' root growth and development are highly dependent on the physical state of the soil (Aluko and Koolen, 2000). To preserve the beneficial characteristics thereof, it is nec-

essary to use suitable agricultural tools that will ensure proper tillage and prevent soil degradation (Kim *et al.*, 2020). Tillage operations are used to create suitable conditions for the growth and rooting of agricultural products and to eliminate weeds (Kraska *et al.*, 2014; de Lima *et al.*, 2022). A softer and more stabilized bed around the seed is considered a proper seed substrate (Losini *et al.*, 2022).

Tillage operations entail loosening and mixing the soil mechanically to provide a better bed for crop production exerting a beneficial effect on soil properties such as soil moisture retention, soil ventilation for proper temperature, and soil permeability development (Busari *et al.*, 2015; Wilczewski *et al.*, 2023).

Draught resistance is one of the most important factors in the interaction between tractor and agricultural implements and plays an essential role in the management thereof. By having data on draught resistance and predicting it in agricultural conditions, agricultural machinery engineers can choose the right tractor and tool with the highest energy efficiency. The draught of tillage implements is a function of soil parameters such as moisture content, soil texture, *etc.*, tool parameters such as depth, angle of attack, blade sharpness, *etc.*, and operational parameters such as tool advancement speed which may change in different

conditions. To calculate and predict the draught resistance, the relationship between the aforementioned parameters should be determined (Abbaspour-Gilandeh *et al.*, 2016).

Proper operational management is a key factor for reducing costs and saving energy. A better understanding of the interaction between tillage tools and the soil can help designers to increase energy efficiency in tillage operations. Accurate simulation of blade-soil interactions can also reduce the need for in-situ tests. In addition, by choosing the appropriate simulation model, the time needed to prepare the appropriate model can be reduced. With the development of computer science, numerical methods have become available in studying interactions between soil and cutting tools. Simulation helps to understand tillage phenomena and predict the applied forces (Azimi-Nejadian *et al.*, 2019).

Azimi Nejadian *et al.* (2019) used the finite element method (FEM) and combined statistical models to predict the force components in the mouldboard plough. Using a 3D-FEM model of the interaction between the soil and the plough, the longitudinal, lateral, and vertical draught components of the mouldboard plough were predicted for the moisture range of 22-30% and dry bulk density of 1 150-1 770 kg m<sup>-3</sup> in sandy loam soil. To validate the simulation, the draught computed with the FEM was compared with experimental data as well as draught forces calculated using the analytical model proposed by Godwin *et al.* (2007). Regression models were developed for the draught prediction. For example, for traction, a model with  $R^2 = 0.82$  and RMSE = 0.78 kN was obtained. The measured draught was 3-9.5 and 4-17% greater than the simulated and analytically calculated draught, respectively. This shows that the developed FEM and statistical models can be used as a simple and useful method of estimating the forces exerted on mouldboard plough components under different combinations of soil physical properties and operating parameters.

Ibrahmi *et al.* (2014) used the FEM to investigate the interaction between the tool and the soil in a three-dimensional model developed using Abaqus Explicit. The soil was modelled using the linear form of the Drucker-Prager model to simulate the shear force. The soil simulation covered various parameters required by the FEM, including Young's modulus ( $E$ ), Poisson's ratio ( $\nu$ ), soil bulk density ( $\rho$ ), yield stress ratio in triaxial tension to triaxial compression ( $k$ ), friction angle ( $\phi$ ), and the dilation angle ( $\psi$ ) for plastic flow. In addition, damage and failure characteristics were used in the property module to simulate soil failure. During the soil cutting process, Abaqus Explicit removed failing elements from the mesh. The tine forward speed was 1 m s<sup>-1</sup> in all the analyses. The study investigated the effects of tillage depth and tine width and it was found that the values of draught and vertical force increased linearly with a slope of 0.037 and 0.0143, respectively, as the tine width increased. A narrow tool (width < 60 mm) had a greater effect on specific draught than a wide tool. Draught and

specific draught force increased in a polynomial and linear curve relative to depth, respectively. In the second part of the study, the authors focused on the diagonal position of the tine to evaluate the impact of the rake angle on the force component of the tiling tool, including tension, lateral and vertical, and the soil cutting process during and after its failure. For all angles considered, the draught force was higher compared to the vertical and lateral forces. It was found that, using small tines at average rake angles of 30 – 45, the most efficient loosening of the soil can be achieved.

Abo-Elnor *et al.* (2004) investigated the effect of the mesh size in the 3D FEM. Draught force was calculated for different mesh densities of the soil using the same tillage conditions. It was determined that the mesh density (proportionate to the number of elements) had an important effect on the tillage forces computed using the numerical model. Bentaher *et al.* (2013) investigated the progress of the tillage tool in relation to a number of different elements and found that the mesh density significantly influenced the prediction of tillage tool forces.

Based on the conducted literature review, it was found that there is no extensive research on the development and distribution exerted stress in front of the cutting tool. Hence, the novelty of the present study is the demonstration of the stress distribution in the soil during soil cutting using the FEM method. Therefore, the objective of this study was to simulate soil cutting by employing the FEM method in an Abaqus Explicit environment. The study also aimed to evaluate the effects of different parameters, such as tool forward speed, working depth, and tool's depth/width ratio, on soil stress as well as the required draught force.

## 2. MATERIALS AND METHODS

Field experiments were conducted to measure and evaluate a number of predetermined parameters. The measured data were then processed with Abaqus 2020 software to evaluate obtained simulation data. Four types of narrow blades with different widths of 2.5, 3, 3.5, and 4 cm and the length of 1 m were used. Field trials were conducted in clay loam soil under a factorial experiment based on a randomized complete block design (RCDB) with three replications. The experimental data were analysed using SpSS21 software (SpSS., 2012). The soil moisture was 15%, and four tractor forward speeds of 1, 1.5, 1.8, and 3 km h<sup>-1</sup> and tine widths of 2.5, 3, 3.5, and 4 cm at working depths of 10, 20, 30, and 40 cm were tested to determine the required draught. The soil moisture was measured with the standard cylinder method after irrigation on different days, and the field experiments were performed once the soil moisture reached 15%. A single differential MF-285 tractor with 56 kW was used to conduct the trials.

To measure the draught force, a three-point connection dynamometer was used (Fig. 1). The dynamometer consisted of an inverted U-shaped frame mounted between

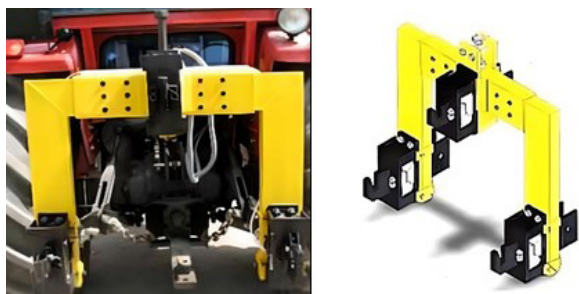


**Fig. 1.** Three-point hitch dynamometer.

the arms of the three-point connection system of the tractor and the agricultural implement. The three-point connection dynamometer was designed in a way that allowed the height of the mid connection rod and the distance between the lower connection points to be adjusted so that it could be easily mounted between the tractor and different agricultural tools. It facilitated the measurement of horizontal and vertical forces exerted on the connection points of the three-point connection system of the tractor. The force sensing unit consisted of three octahedral force transducers incorporated as elastic elements between the inverted U-shaped frame and the dynamometer quick coupling system.

An additional wheel was used to measure the forward speed of the tractor. The constituent parts of this mechanism included a pneumatic tire 39 cm in diameter, which rotated easily on its axis and was positioned in line with the movement of the front wheel of the tractor with the help of various parts of the chassis. The wheel was also equipped with an inductive proximity sensor pr12-2dn from Autonics. The sensor monitored the gear installed in the centre of the fifth wheel and produced a pulse for each tooth movement. The generated pulses were displayed by pulse meters installed inside the tractor cabin. These pulse meters worked with 230 V alternating current. A DC to AC current converter was used to provide the required power of the pulse meter. By dividing the total number of pulses by the total number of gear teeth, the number of full revolu-

tions of the tractor wheel was computed. By multiplying the number of tire rotations by its circumference, the theoretical speed was calculated (Fig. 2).

A DT800 data logger with programming capability from DataTaker was used to store data from the force transducer and penetration depth measurement sensor. Data logger DT800 has 16 digital channels and 12 analogue channels operating using 12 volt direct current (Fig. 3). To ensure that the tines had sufficient resistance against wear and bending, they were manufactured from CK-45 steel standard DIN 17200 grade C45/1.1191. The tines were mounted on a solid chassis during the field tests. The chassis was fitted with depth control wheels to conduct the tillage operations at the desired depths (Fig. 4).



**Fig. 2.** Rreal speed measurement system of the tractor (fifth wheel).



**Fig. 3.** DT800 data logger.



**Fig. 4.** Tillage blades and chassis used in the study.



## 2.1. Finite element method

The performance of soil tillage implements depends primarily on the physical and mechanical properties of the soil. The soil environment depends on the complex balance between the three phases of the soil composition (solid, liquid, and gas), which determines a number of different physical and chemical processes responsible for the mechanical behaviour of the soil. The mechanical properties of the soil during loading and unloading are reflected by its elastic and plastic deformation with a non-linear change. In the presented study, the Drucker-Prager method was used for the purposes of soil modelling. In order to model soil in Abaqus software (Abaqus, 2020), parameters such as the modulus of elasticity ( $E$ ), Poisson's ratio ( $\nu$ ), Drucker-Prager internal friction angle ( $\beta$ ), stress flow ratio ( $K$ ), and dilation angle ( $\psi$ ) need to be input. A uniaxial test was performed to obtain Poisson's ratio of  $\nu$  and modulus of elasticity, while a triaxial test provided data on the soil internal friction angle ( $\varphi$ ) and soil cohesion ( $c$ ). The Drucker-Prager model and its extended form are used to simulate the behaviour of soil, particularly where the material performance is associated with hardening. Different forms of performance levels can be observed in the Drucker-Prager model. It can have linear, hyperbolic, or general exponential forms (Drucker and Prager, 1952). In the present study, the soil was modelled as a continuous elasto-plastic material with the hardening property using the linear form of the developed Drucker-Prager model. This model can be defined as follows:

$$F_s = t - p \tan \beta - d = 0, \quad (1)$$

$$t = \frac{1}{2} q \left\{ 1 + \frac{1}{K} - \left( 1 - \frac{1}{K} \right) \left( \frac{r}{q} \right)^3 \right\}, \quad (2)$$

$$q = \sigma_1 - \sigma_3, \quad (3)$$

$$p = \frac{1}{3} (\sigma_1 + \sigma_2 + \sigma_3), \quad (4)$$

$$r^3 = -(\sigma_1 - \sigma_3) = -q^3. \quad (5)$$

In these relationships,  $F_s$  is the yield function,  $t$  is the deviatoric stress,  $p$  is the average stress,  $\beta$  is the Prager angle of internal friction,  $d$  is the material cohesion,  $q$  is the average Von Mises stress,  $K$  is the flow stress ratio,  $r$  is the third invariant of the deviatoric stress, and  $\sigma_1$ ,  $\sigma_2$ , and  $\sigma_3$  are the compressive stress values obtained in the triaxial test. The flow stress ratio ( $K$ ) is the ratio of yield stress in triaxial tension to yield stress in triaxial compression and, as such, determines the dependence of the yield surface on the value of the intermediate principal stress, which varies from 0.778 to 1 (Drucker and Prager, 1952). For  $K=1$ , the extended Drucker-Prager model becomes the primary

Drucker-Prager model (Farhadi *et al.*, 2019).  $K$  can be calculated by using Mohr-Coulomb's internal friction angle from Eq. (6):

$$K = \frac{3 - \sin \varphi}{3 + \sin \varphi}. \quad (6)$$

To calculate the material cohesion and the internal friction angle in the Drucker-Prager behaviour model in the triaxial stress conditions, the parameters of shear strength in the Mohr-Coulomb model can be obtained from Eqs (7) and (8):

$$\tan \beta = \frac{6 \sin \varphi}{3 - \sin \varphi}, \quad (7)$$

$$d = \frac{18c \cos \varphi}{3 - \sin \varphi}. \quad (8)$$

In these relationships,  $c$  and  $\varphi$  are the soil cohesion and internal friction angle in the Mohr-Coulomb model, and  $\beta$  and  $d$  are the internal friction angle and cohesion of material in the Drucker-Prager model, respectively (Drucker and Prager, 1952).

When modelling a perfectly elastic plastic material without hardening, the compressive yield stress  $\sigma_c$  can be calculated from the cohesion  $c$  and  $\varphi$ :

$$\sigma_c = 2c \frac{\cos \varphi}{1 - \sin \varphi}. \quad (9)$$

The dilatation angle  $\psi$  determines the direction of the slope of the plastic strain  $de^{pl}$  relative to the yield surface and expresses the two laws of plastic flow (associated flow and non-associated flow) (Drucker and Prager, 1952). The results of associated flow with the  $\psi=\beta$  setting (*i.e.* the direction of plastic strain perpendicular to the yield surface) were used in this study (Rahmatian *et al.*, 2021).

The complete results illustrating the mechanical properties of the studied soil, which was a clay loam type, at 15% moisture are given in Table 1. The soil parameters for the Drucker-Prager model were measured at this moisture content, and then the resulting soil properties were inputted into the Abaqus 2020 software.

**Table 1.** Physical and mechanical characteristics of the studied soil

Parameter	Value
Young's modulus, $E$ (MPa)	4.02
Poisson's ratio, $\nu$	0.43
Density, $\rho$ (kg m <sup>-3</sup> )	1315
Cohesion, $c$ (MPa)	0.035
Internal angle of friction of soil, $\varphi$ (°)	16.43
Flow stress ratio, $K$	0.82
Dilation angle, $\psi$	32
Drucker-Prager internal angle of friction, $\beta$ (°)	32
Soil and metal coefficient of friction, $\delta$ (°)	0.5
Compressive yield stress, $\sigma_c$ (MPa)	0.09362

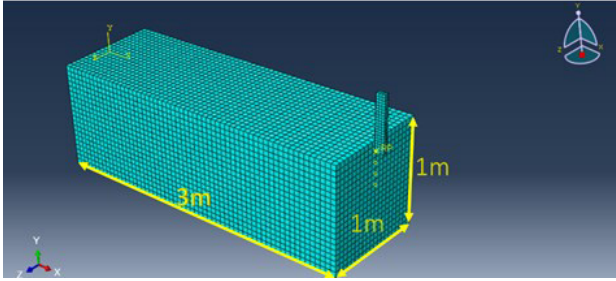


Fig. 5. 3D model of soil and blade.

## 2.2. Soil and tillage tool modelling

In order to investigate the effect of the depth/width ratio and the forward speed of the narrow tine on the soil stress and draught force, a three-dimensional model was prepared (Fig. 5). The model consisted of two distinct Abaqus parts: 1) a deformable soil box: a box 3 m in length, 1 m in width, and 1 m in depth, and 2) a rigid tine: a rigid and discrete body with the length ( $L$ ) and width ( $w$ ). For the rigid body, there was no need for defining and applying any material because its parameters are not extracted in the Results section. A reference node was assigned to the blade in order to apply boundary conditions. The soil-blade contact was defined in a contact step. Surface to surface contact (explicit) was used to define the parts of the blade and soil that were in contact with each other. Given that the modulus of elasticity of the tine was higher than that of the soil, the tine was selected as the master and the soil that was selected as the slave. Furthermore, the formulation of the mechanical constraint penalty contact method was used to define the desired interaction. To include internal elements in this constraint, rather than select the soil surface, all the elements in contact with the tine surface were selected as the slave. Simulation was done with the dynamic explicit solution method. The dynamic explicit method is suitable for problems where the total kinetic energy of the model is greater than 0.01 of the total energy (Drucker and Prager, 1952). The boundary condition of the soil box was a constant dis-

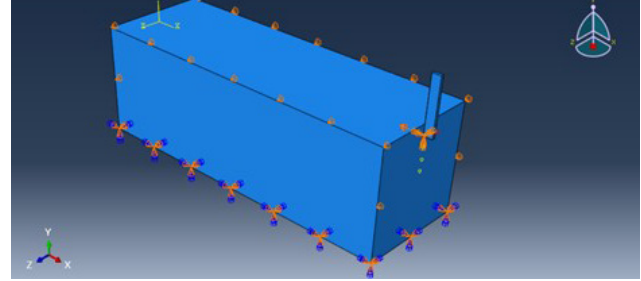


Fig. 6. Applying boundary conditions to the soil box and applying velocity to the reference point of the blade.

placement in the direction perpendicular to each surface. This was applied in the right, left, and bottom planes. The front and rear parts and the upper surface had freedom of movement (Fig. 6). In the load step of the software, different speeds of 1, 1.5, 1.8, and 3 km h<sup>-1</sup> were applied to the tine in the direction of X on the reference point of the tine, and the other five degrees of freedom were fixed. To avoid deviation from the calculation algorithm, the tool should reach this speed gradually. The soil cutting was done at the depths of 10, 20, 30, and 40 cm.

The studied soil was clay loam with the density of 1315 kg m<sup>-3</sup> and moisture content of 15% (d.b.) with Young's modulus of 4.02 MPa, Poisson's ratio of 0.43, a Drucker-Prager internal friction angle of 32°, and soil cohesion of 0.035 MPa. The soil was meshed with 8-node linear Eulerian cubic elements with reduced integral and hourglass control (C3D8R), and the body of the narrow tillage blade, which was considered rigid, was meshed with 8-node linear cubic elements with reduced integral and hourglass control (C3D8R).

The explicit method is used in the Abaqus software, which can simulate large deformations with connected Eulerian-Lagrangian analysis. Abaqus/Explicit performed a fully dynamic analysis. In this analysis, the tine was modelled as Lagrangian and the soil as Eulerian. The soil was assumed to be fully elastic-plastic. The three-dimensional model of the soil and the meshed blade shows the soil cut (Fig. 7). The cutting of the soil was such that when

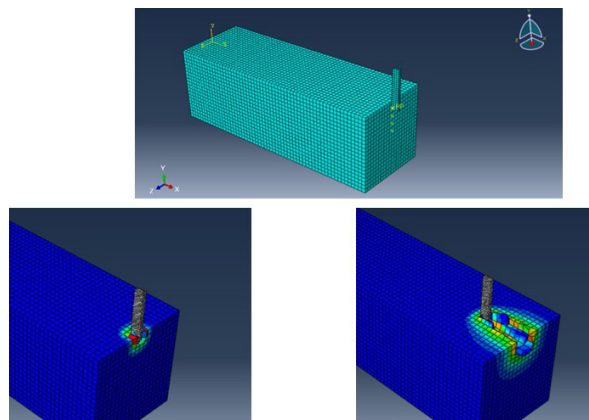


Fig. 7. 3D model of soil and meshed blade, soil in front of the blade and the stress exerted on the soil.

the amount of stress exceeded the limit determined in the material properties section, the elements were automatically removed.

### 2.3. Number of elements and nodes

The dimensions of the element have a direct effect on the convergence of the results of the problem, so they must be determined accurately. If the size of the elements is small, *i.e.* closer to the size of the soil texture, a more accurate final result will be obtained. However, smaller elements simultaneously increase the calculation time. The size of the elements, accuracy, and number of degrees of freedom of the researched material depend on the number of elements determined for the simulation. Better results can be obtained with an increasing element number; however, for each subject, there is a certain limit in terms of the number of elements beyond which the accuracy of the result cannot be improved significantly. Hence, the number of elements started from 20 000 for the soil and increased by almost 2 000 in each stage. It was found that there was no significant difference between 26 000 and 24 000 elements in terms of the obtained results. Then, the 24 000 value was accepted as an optimum mesh value based on the results of the accuracy and computing time. Table 2 presents both the optimum element and node numbers for the tine and soil parts.

## 3. RESULTS AND DISCUSSION

### 3.1. Evaluation of the simulation results against experimental data

Table 3 shows some descriptive and statistical parameters, such as the mean draught value, standard deviation, and mean standard error, obtained in the field experiments

**Table 2.** Number of elements and nodes of the soil and blade

Number	Soil	Tillage blade
Element	24000	833
Node	26901	1377

**Table 3.** Some statistical parameters of draught data from field trials and Abaqus simulations

Source of changes	Number	Average	Standard deviation	Mean standard error
Field experiments	64	9.1664	3.63177	0.45397
Abaqus models	64	8.9462	3.35237	0.41905

**Table 4.** T-test to check mean differences between experimental and FEM simulation data

$t$	Degrees of freedom	Significant level	Difference of the averages	Standard error difference	95% confidence level	
					Min.	Max.
0.356	126	0.722	0.22016	0.61781	-1.0024	1.4427

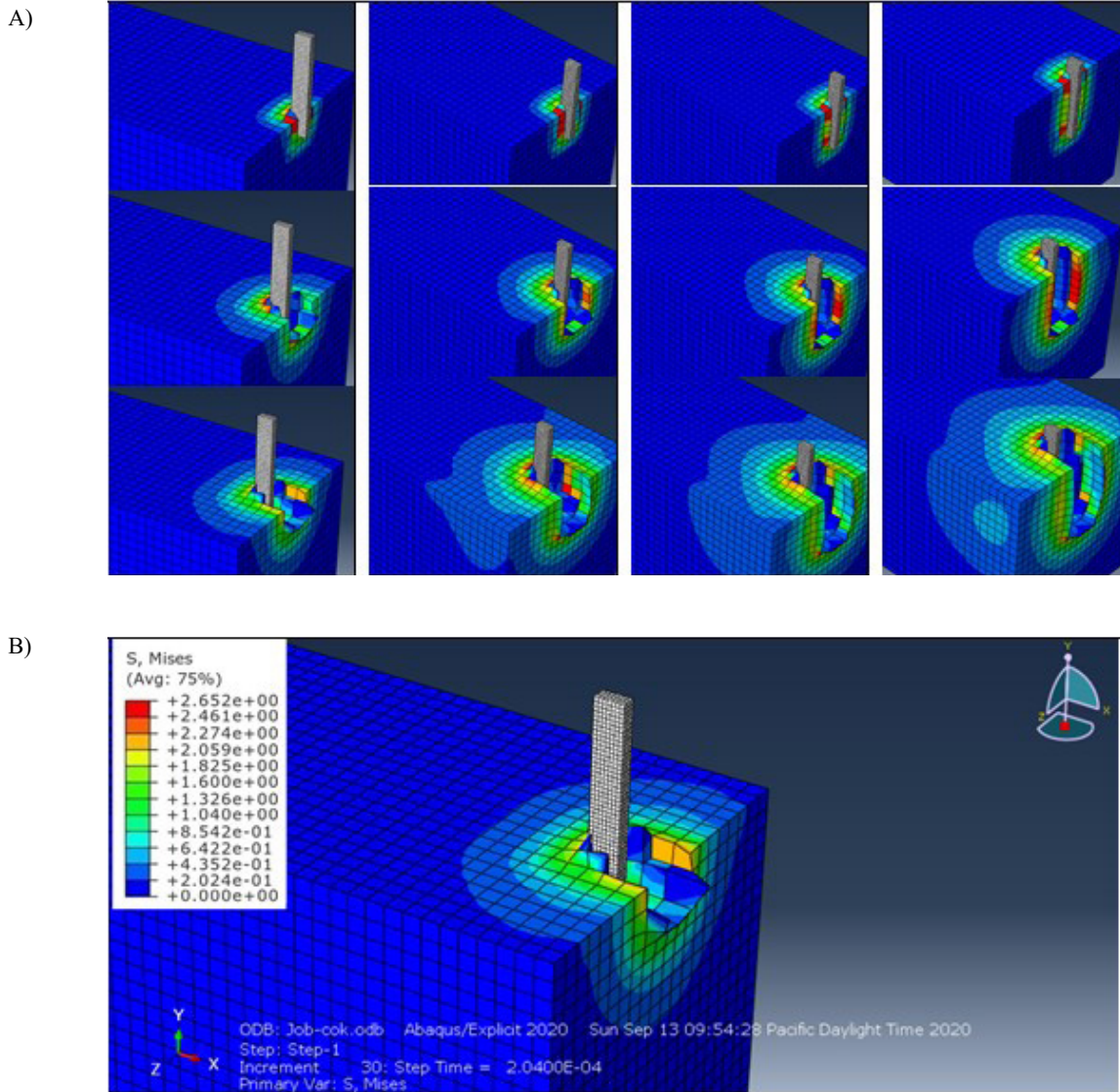
and respective Abaqus models created in conditions similar to the field trials in terms of tool parameters and operating conditions using SpSS 21 software.

Table 4 shows that the t-test was used to compare the draught force data obtained from the trials and the FEM simulation, and since the calculated significance level was greater than 0.05, the difference between the means was not significant. This shows that the FEM simulation results are in good agreement with the experimental results. Bases on stress results when the mouldboard ploughed the soil, Bentaher *et al.* (2013) indicated that the developed FEM model simulated the cutting process perfectly. Abo-Elnor *et al.* (2004) concluded that 3D FEM modelling is a suitable method for describing the concept of soil failure in soil-blade interaction problems. Then, the results and discussion presented in the rest of the paper relate to the FEM simulation data.

### 3.2. Maximum stresses exerted on the soil

Figure 8A presents the respective stages of cutting the soil at different depths with a tine of 2.5 cm in width. The maximum stress (Fig. 8B) was observed at the depth of 10 cm and the speed of 3 km h<sup>-1</sup>. The stress plot in Figs 7 and 8 revealed no stress and soil compaction at the bottom of the tine. This was due to the lack of a cutting wedge at the bottom of the tine. If a wedge is present, it exerts vertical force of the tine, which compresses the bottom of the furrow. A wedge creates considerable tension at the bottom of the furrow and causes soil compaction when tillage operations are carried out at the same depth for many years (Nisha *et al.*, 2023).

Figure 9 shows the effect of increasing the  $d/w$  ratio at different forward speeds on the stress exerted on the soil. It was also found that, as the forward speed increased at the different  $d/w$  ratios, so did the stress exerted on the soil. Other researchers also reported that the required draft increased significantly with a higher tillage tool speed (Askari *et al.*, 2016; Moeinfar *et al.*, 2014). Similarly, Askari *et al.* (2016) found that with an increasing advance speed, both the draft and the specific draft requirements increased. The stress increase with the increasing forward speed was consistent with previous research reports. Moreover,



**Fig. 8.** A) Soil cuts at the depth of 10, 20, 30 and 40 cm time points of forward movement, B) the maximum amount of stress was exerted on the soil at the depth of 10 cm by the blade of 4 cm in width moving at the speed of 3 km h<sup>-1</sup>.

the speed increase accelerated soil failure as acceleration increased the stress exerted on the soil. Hence, the increase in the draft with the speed was the result of stress increment. The effect of the speed increase on stress increment was more significant at the shallow depth of 10 cm, compared to the higher depths of *e.g.* 40 cm. It was also found that the increasing tilling depth had a reverse effect on the generated stress. Figure 9 shows that the increasing *d/w* ratio at all the advancing speeds reduced the stress observed in the soil at the beginning of failure. Increasing both the forward speed and the tilling depth increased the force required for soil failure. At low *d/w* ratios at which crescent failure occurred, maximum stress was exerted on the front and top soil. At the same time, where with the

increasing *d/w* ratio the depth exceeded the critical value, the total stress was distributed between the crescent and lateral manners. Consequently, the overall stress decreased with the *d/w* ratio increment.

**3.3. Effect of working depth, tine width, and forward speed on draught**

The data obtained from the simulation of soil cutting with a narrow tine revealed that, by increasing the tilling depth from 10 to 20 cm (Fig. 10A), the draught force of the blade increased for the tine of 2.5 cm in width and movement speed of 1 km/h. Moreover, as shown in Fig. 10B, when the forward speed of the tractor increased from 1 to 1.5 km h<sup>-1</sup> at the constant tine width and tilling depth, the draught force also increased.

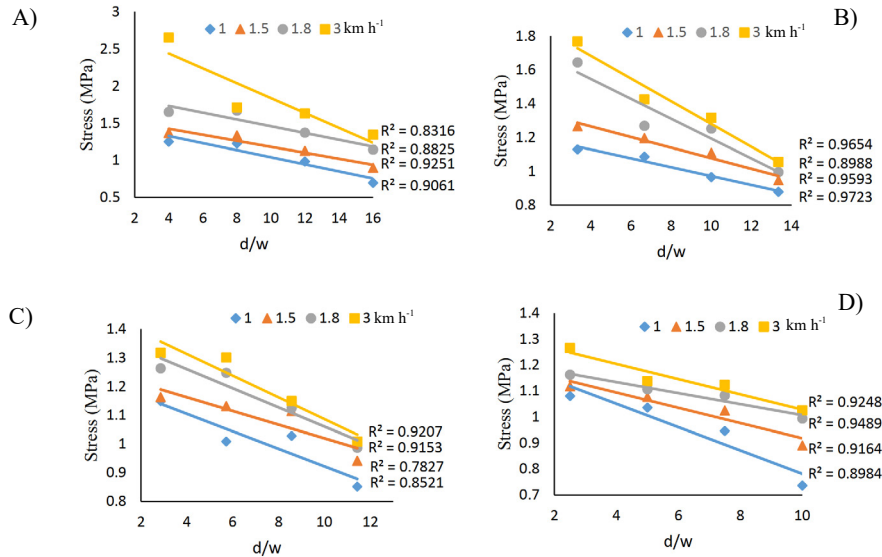


**Fig. 9.** Effect of increasing the  $d/w$  ratio at different forward speeds on the amount of stress exerted on the soil by blades width of: A) 2.5 cm, B) 3 cm, C) 3.5 cm, D) 4 cm in width, respectively, at all tillage depths.

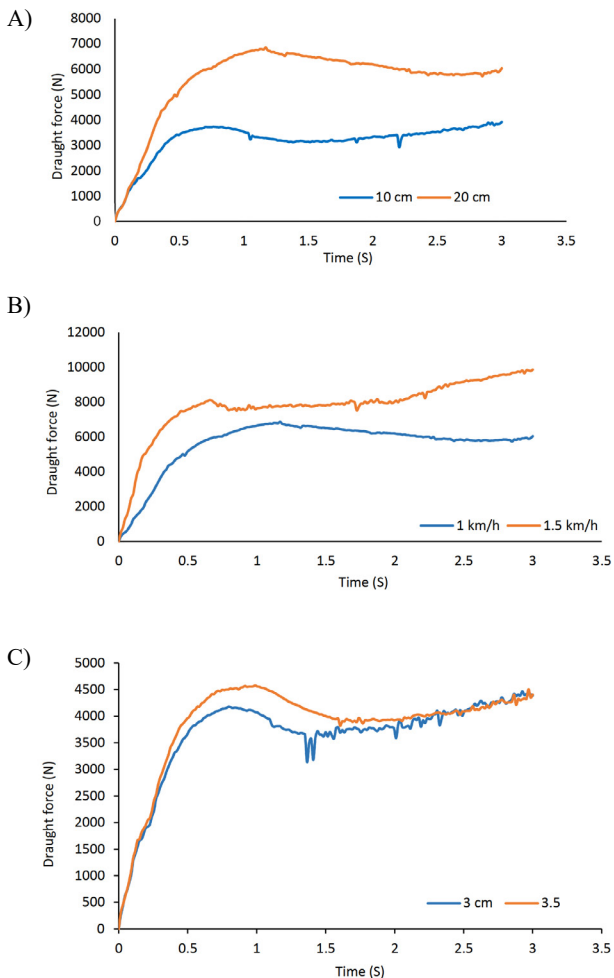


**Fig. 10.** Draught force variations for the narrow tillage blade, data obtained from the software: A) 2.5 cm blade at the depth of 10 and 20 cm at 1 km h<sup>-1</sup>, B) 2.5 cm blade at the depth of 20 cm at 1 and 1.5 km h<sup>-1</sup>, C) 3 and 3.5 cm blade at the depth 10 cm at 1 km h<sup>-1</sup>.

Furthermore, according to Fig. 10C, when the tine width changed from 3 to 3.5 cm at the velocity of 1 km h<sup>-1</sup> and the depth of 10 cm, the draught force increased. Abbaspour-Gilandeh *et al.* (2005) studied the effect of three independent variables, including ploughing depth of 10, 15, and 20 cm, rake angle of 60, 75, and 90°, and forward speed of 0.5, 1, 1.35, and 1.7 m s<sup>-1</sup>, on the draught induced by a narrow tine. The results showed that the draught force of the narrow tine with increasing tillage depth, the angle of attack, and the speed of the traction increased.

This increase in draught with the tillage depth may have been due to the greater area of interaction between the tine involvement and the fact that larger volumes of soil were cut and displaced, which in turn increased soil mechanical resistance (soil cone index). In addition, the increase in inertial forces due to the need to accelerate a greater mass of soil increased the force of the soil's reaction to the tine (Al-Suhaibani and Ghaly, 2010). Figure 11 shows the triple interaction effect between the forward speed, depth, and tine width on the draught resistance of the vertical narrow tillage tine relative to the results obtained from the field data and the simulated model.

The data collected in Figure 11 show that the draught resistance increased significantly at the increased working depths, speed of advance, and width of the tillage blade. The draft increase was 57, 34, and 19.5% as the working depth increased from 10 to 20, from 20 to 30, and from 30 to 40 cm, respectively. A maximum increase of 21% occurred as the travel speed increased from 1 to 1.5 km h<sup>-1</sup>. The two other increase percentages were 2.2 and 3.4%, respectively. Askari *et al.* (2017) investigated the effect of tine, speed, depth, and wing of addition on the draft required in subsoil tillage tines from three levels of tine (*i.e.* subsoiler, paraplough, and bentleg), four levels of speed



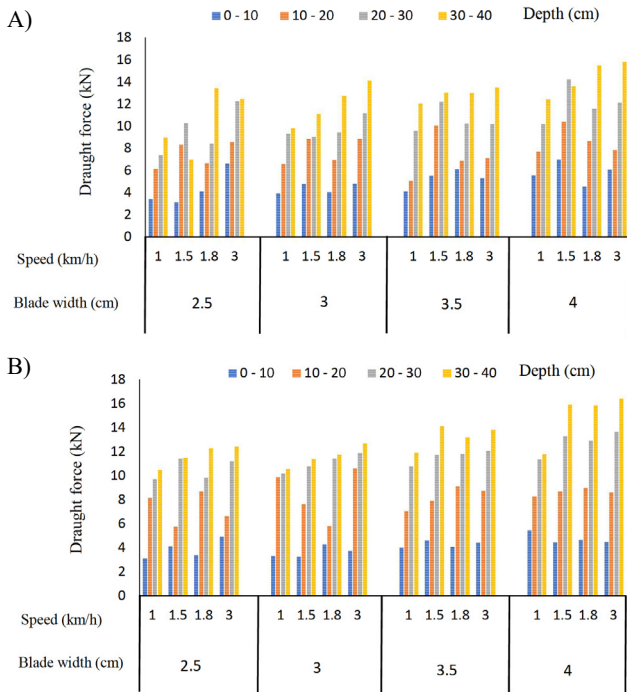


**Fig. 11.** Bar graph of the triple interaction effect between the forward speed, depth and blade width on the draught resistance of the vertical narrow tillage blade: A) results obtained from the field experiment and B) results obtained from the simulated model.

(i.e. 1.8, 2.3, 2.9, and 3.5 km h<sup>-1</sup>), three depth levels (i.e. 30, 40, and 50 cm), and two wing levels (i.e. wingless and winged blades). Upon the increase in the forward speed and ploughing depth and the addition of wings the draft required in all the tines increased. The highest amount of draft force is related to the winged subsoiler at a depth of 50 cm and a speed of 3.5 km h<sup>-1</sup>, and the lowest is related to the bentleg base at a depth of 30 cm and a speed of 1.8 km/h.

**3.4. Comparison of the relationship between draught and forward speed at different depth/width ratios**

The results indicate that, after the acceleration of the forward speed from 1 to 3 km h<sup>-1</sup>, the draught force increased for all the analysed depth/width ratios, and the linearity of each of the depth/width ratios can be seen in the graph (Fig. 12).

As the depth/width ratio increased with the decrease in the tine width, the draught force value was the lowest at the depth/width ratio of 4. These depth/width ratios are presented from right to left for the depths of 10, 20, 30, and 40 cm and the widths of 2.5, 3, 3.5, and 4 cm, respectively. The lowest draught force of 3.13 kN was recorded for the depth/width ratio of 4 and corresponded to the ploughing depth of 10 cm, the blade width of 2.5 cm, and the forward speed of 1 km h<sup>-1</sup>. The maximum draught force of 15.81 kN was

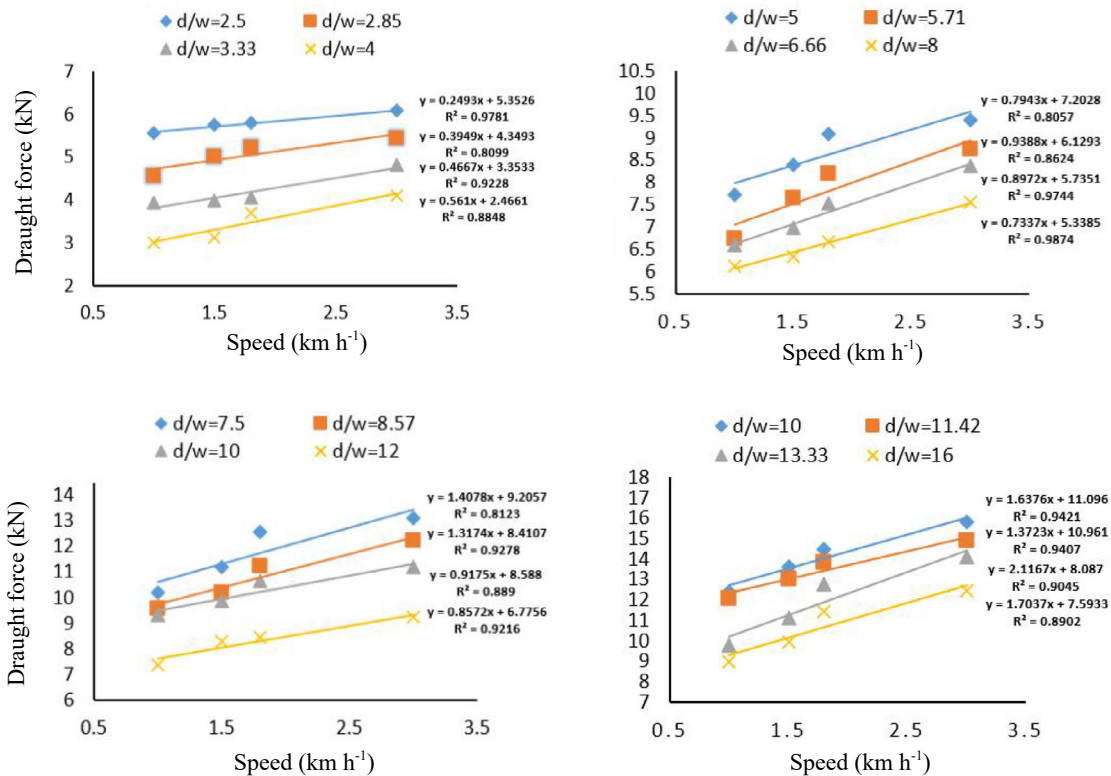


**Fig. 12.** Relationship between draught force and forward speed at the depth to width ratios of 2.5-16 in the 437 simulated model.

recorded for the depth/width ratio of 10, corresponding to the tillage depth of 40 cm, the blade width of 4 cm, and the forward speed of 3 km h<sup>-1</sup>.

#### 4. CONCLUSIONS

1. The draught force data obtained from the field experiments and the finite element method simulation revealed good agreement between the 3D Fem simulation and field test results. Hence, it was found that the developed model was reliable in simulating soil behaviour during cutting operations using a tillage tool.

2. The field test showed that the main factors affecting the draught strength of the vertical narrow blade were the tool's forward speed, tillage depth, and tine width. Their effects as well as their double and triple interaction effect on the draught force were significant at the probability level of 1%.

3. The maximum stress of 2.62 MPa was exerted on the soil at the depth of 10 cm and the travel speed of 3 km h<sup>-1</sup>. The stress increased with the increasing forward speed. The speed increase accelerated soil failure, and then increased the stress exerted on the soil. Hence, the increase in the draft with the speed was the result of stress increment. The effect of the speed increase on stress increment was more significant at the shallow depths of 10 cm compared to higher depths. The increase in the depth/width ratio reduced the exerted stress in the soil.

4. Both the experiments and the finite element method simulation showed that, in all the evaluated conditions, increasing the tillage depth from 0 to 40 cm and increasing the forward speed from 1 to 3 km h<sup>-1</sup> increased the required draught force. At the same time, increasing the width of the blade increased the mechanical resistance of the soil and, as a result, also the draught required increased. Draft values of 7.9, 8.5, 9, and 10.21 kN were reported at the different widths of 2.5, 3, 3.5, and 4 cm, respectively. The maximum draft increment of 13.5% occurred as the width of the tines increased from 3.5 to 4 cm.

**Conflicts of Interest:** The Authors do not declare any conflict of interest.

#### 5. REFERENCES

- Abaqus, Abaqus User's Manuals Version. Dassault Systèmes Simulia Corp., Providence, RI, 2020.
- Abbaspour-Gilandeh, Y., Khalifeh, A.A., Ghavami-Jolandan, S., 2016. Evaluation of factors affecting the draft of a curved shape subsoiler and prediction of its draft using multiple variables regression model. *J. Soil Sci. Sgric. Eng.* 38, 95-110. <https://doi.org/10.22055/AGEN.2016.11668>
- Abbaspour-Gilandeh, Y., Khalilian, A., Reza A., Alireza, K., Sadati, S., 2005. Energy savings with variable-depth tillage, Proc. 27th Southern Conservation Tillage Systems Conf., Florence, South Carolina, USA, June 27-29. North Carolina Agricultural Research Service, North Carolina State University, 84-91.
- Abo-Elnor, M., Hamilton, R., Boyle, J., 2004. Simulation of soil-blade interaction for sandy soil using advanced 3D finite element analysis. *Soil Till. Res.* 75, 61-73. [https://doi.org/10.1016/S0167-1987\(03\)00156-9](https://doi.org/10.1016/S0167-1987(03)00156-9).
- Al-Suhaibani, S., Ghaly, A.E., 2010. Effect of plowing depth of tillage and forward speed on the performance of a medium size chisel plow operating in a sandy soil. *Am. J. Agric. Biol. Sci.* 5, 247-255. <http://dx.doi.org/10.3844/ajabssp.2010.247.255>.
- Aluko, O., Koolen, A., 2000. The essential mechanics of capillary crumbling of structured agricultural soils. *Soil Till. Res.* 55, 117-126. [https://doi.org/10.1016/S0167-1987\(00\)00105-7](https://doi.org/10.1016/S0167-1987(00)00105-7).
- Askari, M., Shahgholi, G., Abbaspour, Y., Shamsabadi, H.T., 2016. Effect of forward speed and tillage depth on tractor-subsoiler performance. *J. Agric. Eng. Res.* 16(65), 109-128. <https://doi.org/10.22092/erams.2016.105958>.
- Askari, M., Shahgholi, G., Abbaspour-Gilandeh, Y., 2017. The effect of tine, wing, operating depth and speed on the draft requirement of subsoil tillage tines. *Res. Agr. Eng.* 63(4), 160-167. <https://doi:10.17221/4/2016-RAE>
- Azimi-Nejadian, H., Karparvarfard, S.H., Naderi-Boldaji, M., Rahmanian-Koushkaki, H., 2019. Combined finite element and statistical models for predicting force components on a cylindrical mouldboard plough. *Biosyst. Eng.* 186, 168-181. <https://doi.org/10.1016/j.biosystemseng.2019.07.007>.
- Bentaher, H., Ibrahim, A., Hamza, E., Hbaieb, M., Kantchev, G., Maalej, A., *et al.*, 2013. Finite element simulation of moldboard-soil interaction. *Soil Till. Res.* 134, 11-16. <https://doi.org/10.1016/j.still.2013.07.002>.
- Busari, M.A., Kukal, S.S., Kaur, A., Bhatt, R., Dulazi, A.A., 2015. Conservation tillage impacts on soil, crop and the environment. *Soil Water Conserv. Res.* 3, 119-129. <https://doi.org/10.1016/j.iswcr.2015.05.002>
- de Lima, C.C., De Maria, I.C., da Silva Guimarães Júnnyor, W., Figueiredo, G.C., Dechen, S.C.F., Bolonhezi, D., 2022. Root parameters of sugarcane and soil compaction indicators under deep strip tillage and conventional tillage. *Sci. Rep.* 12, 18537. <https://doi.org/10.1038/s41598-022-21874-1>
- Drucker, D.C., Prager, W., 1952. Soil mechanics and plastic analysis or limit design. *Q. Appl. Math.* 10, 157-165.
- Farhadi, P., Golmohammadi, A., Malvajardi, A.S., Shahgholi, G., 2019. Finite element modeling of the interaction of a treaded tire with clay-loam soil. *Comput. Electron. Agric.* 162, 793-806. <https://doi.org/10.1016/j.compag.2019.05.031>
- Godwin, R.J., O' Dogherty, M.J., Saunders, C., Balafoutis, A.T., 2007. A Force prediction model for Mouldboard Plough incorporating the effects of soil characteristics properties, plough geometric factors and ploughing speed. *Biosyst. Eng.* 97, 117-129. <https://doi.org/10.1016/j.biosystemseng.2007.02.001>
- Ibrahim, A., Bentaher, H., Maalej, A., 2014. Soil-blade orientation effect on tillage forces determined by 3D finite element models. *Span. J. Agric. Res.* 12, 941-951. <http://dx.doi.org/10.5424/sjar/2014124-5766>.
- Kim, Y.S., Kim, T.J., Kim, Y.J., Lee, S.D., Park, S.U., Kim, W.S., 2020. Development of a real-time tillage depth measurement system for agricultural tractors: application to the effect analysis of tillage depth on draft force during plow tillage. *Sensors* 20, 912. <https://doi.org/10.3390/s20030912>.

- Kraska, P., Andruszczak, S., Kwiecińska-Poppe, E., Pałys, E., 2014. Tillage systems and catch crops as factors determining weed infestation level in a spring wheat canopy (*Triticum aestivum* L.) sown in monoculture. *Acta Sci. Pol. Agricultura* 13(2), 33-50.
- Lobb, D.A., Huffman, E., Reicosky, D.C., 2007. Importance of information on tillage practices in the modelling of environmental processes and in the use of environmental indicators. *J. Environ. Manag.* 82(3), 377-387.
- Losini, A.E., Grillet, A.C., Woloszyn, M., Lavrik, L., Moletti, C., Dotelli, G., *et al.*, 2022. Mechanical and microstructural characterization of rammed earth stabilized with five biopolymers. *Materials* 15, 3136.  
<https://doi.org/10.3390/ma15093136>.
- Moeinfar, A., Mousavi-Seyedi, S., Kalantari, D., 2014. Influence of tillage depth, penetration angle and forward speed on the soil/thin-blade interaction force. *Agric. Eng. Int.: CIGR J.* 16, 69-74.
- Nisha, K., Upadhyay, G., Patel, B., Sihag, N., Choudhary, S., Rani, V., 2023. Analysis of soil compaction induced beneath the working depth due to tilling action of different active tillage machinery. *Spanish J. Agric. Res.* 21(4), e210.  
<https://doi.org/10.5424/sjar/2023214-20351>
- Rahmatian, M., Nematollahi, A., Yeganeh, R., Sharifi Malvajerdi, A., 2021. Modeling and predicting the relationship between cone index and soil shear strength with draft force of a symmetrical tillage tool. *J. Eng. Res. Agr. Mech. Syst.* 22(77), 101-118.
- SpSS, IBM SPSS Statistics 21 Core System User's Guide, Version 21.0. Armonk, NY: IBM Corp. 2012.
- Wilczewski, E., Jug, I., Lipiec, J., Gałęzewski, L., Đurđević, B., Kocira, A., *et al.*, 2023. Tillage system regulates the soil moisture tension, penetration resistance and temperature responses to the temporal variability of precipitation during the growing season. *Int. Agrophys.* 37(4), 391-399.  
<https://doi.org/10.31545/intagr/171478>